IEEE Photonics Journal
An IEEE Photonics Society Publication

Divided-Pulse Nonlinear Amplification at 1.5 μm

Volume 8, Number 5, October 2016

Qiang Hao
Yunfeng Wang
Tingting Liu
Hong Hu
Heping Zeng

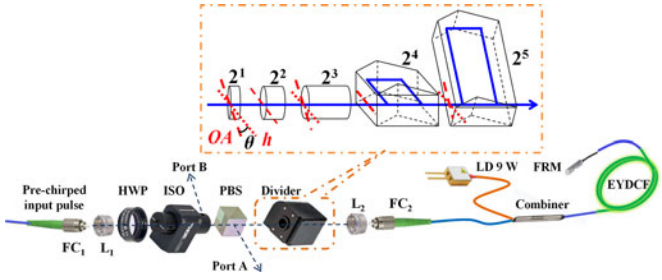

DOI: 10.1109/JPHOT.2016.2603233
1943-0655 © 2016 IEEE

Divided-Pulse Nonlinear Amplification at 1.5 μm

Qiang Hao,[1] Yunfeng Wang,[1] Tingting Liu,[1] Hong Hu,[2] and Heping Zeng[1, 3]

[1]Shanghai Key Laboratory of Modern Optical Systems and Engineering Research Center of Optical Instruments and Systems, Ministry of Education, School of Optical Electrical and Computer Engineering, University of Shanghai for Science and Technology, Shanghai 200093, China.
[2]Department of Respiratory Medicine, Chinese PLA General Hospital, Beijing 100853, China.
[3]State Key Laboratory of Precision Spectroscopy, East China Normal University, Shanghai 200062, China.

DOI:10.1109/JPHOT.2016.2603233

Manuscript received June 10, 2016; revised August 20, 2016; accepted August 22, 2016. Date of publication August 26, 2016; date of current version September 14, 2016. This work was supported in part by the National Key Scientific Instrument Project under Grant 2012YQ150092; in part by the National Natural Science Foundation of China Grant 11404211, Grant 11434005, and Grant 11374370; in part by the Shanghai Municipal Science and Technology Commission under Grant 13ZR1458100; and in part by the Hujiang Foundation of China under Grant D15014. Corresponding author: H. Zeng (e-mail: hpzeng@phy.ecnu.edu.cn).

Abstract: Divided-pulse nonlinear amplification was developed in the anomalous dispersion regime by combining the concepts of divided-pulse nonlinear amplification and divided-pulse compression. We realized compressor-free ultrafast pulse amplifiers at 1.5 μm with the help of simultaneous pulse amplification and compression in single-mode and few-mode fibers with anomalous dispersion. With optimized positive prechirping on the seed pulse, the interplay between the dispersive and nonlinear effects was controlled to get transform-limited soliton replicas. Experiments, as well as numerical simulations, demonstrated that $\sim$0.75 nJ per replica was the optimized results in the 12/130 Er-Yb codoped fiber. By polarization-division multiplexing 32 replicas, transform-limited pulse with 126-fs duration, 20.3-nJ pulse energy, and 80-MHz repetition rate was generated from a few-mode Er-Yb codoped fiber. Furthermore, limitations on the coherent combining efficiency are discussed.

Index Terms: Fiber Lasers, erbium lasers, laser amplifiers, pulse compression.

1. Introduction

High-power and high-energy transform-limited pulses around 1.55 μm are needed for applications such as cataract surgery, frequency comb, THz generation, and nonlinear spectroscopy [1]–[4]. As common fiber laser oscillators provide quite limited output powers, Er-doped fiber amplifiers (EDFAs) are widely used for power amplification. However, broad pedestal and pulse break-up typically occur in high-power EDFAs owe to the interplay between self-phase modulation (SPM) and anomalous dispersion in the small fiber core. Therefore, the development of techniques to overcome the limitations on transform-limited pulse generation around 1.55 μm is still an active area.

Master oscillator power amplifiers normally employ large-mode-area fiber to mitigate optical nonlinearity, photonic-crystal fibers (PCFs) to support single-mode operation, as well as high doping

concentration to contract active fiber length. A laser with 0.3-nJ pulse energy and 0.32-ps temporal duration at a repetition rate of 52 MHz was amplified to 2.3 nJ in a multimode Er-fiber with 16-μm core diameter [5]. Chirped-pulse amplification (CPA) is an alternative way of decreasing pulse peak power as well as avoiding the inherent nonlinearity in fiber amplifiers. However, CPA in EDFA is inevitably accompanied by the gain-narrowing effect and high-order dispersion, and therefore hardly produces ultrashort pulse less than 400-fs temporal duration [6]–[8]. Recently, very-large mode area fibers ($\sim$1000 μm^2 effective area) and high-order mode fibers were demonstrated to be able to boost femtosecond pulse to $\sim\mu$J energy, while the shortest pulse duration was measured to be 491 fs [9], [10]. Though the cladding pump geometry provides higher gain for high-order-mode, the modal dispersion is hardly compensated by pulse compressors [11], [12]. Therefore, high-energy pulse amplification with pulse duration less than 100 fs cannot be expected by infinitely expanding the mode area.

Divided-pulse amplification (DPA) paves an effective way for ultrashort pulse amplification around 1.55 μm [13]–[16]. A single seed pulse is temporally divided into 2^N (N is the stage number of the divider) time-delayed replicas that are equally distributed in two perpendicular polarizations [17]–[19]. When a Faraday rotation mirror is employed at the end of the amplifier, the polarization of the 2^N replicas rotate 90° with respect to the input beam, go through the same gain fiber and the divider sequence twice but in the opposite direction, and, consequently, undergo the same total delay. Ideally, each of these replicas experiences identical laser gain and possesses the same temporal and spectral shape, thus ensuring high efficiency recombination. Without DPA, as much as 42-nJ pulse energy (928-mW average power) is achieved in large-mode-area (LMA) Er-fiber amplifier, but the optimized pulse duration was confined to 650-fs [20]. Besides, another experiment demonstrated that 50-kW peak power within 2-ps duration starts to distort the spectrum in LMA-PCF [17]. Nonlinear pulse compression of temporally divided pulses can provide peak power much higher than the self-focusing threshold [21], [22]. Although divided-pulse ideas were first applied to Yb-fiber amplifier where normal dispersion controlled the nonlinear evolution, it was recently recognized that differential dispersion, non-equal replicas, and depolarization limited the coherent combining efficiency [18], [23].

For DPA at 1.55 μm, ref. [15] demonstrated the possibility of divided-pulse compression in a Er/Yb-codoped fiber amplifier which delivered 12.5-nJ energy and 122-fs duration with the help of 8-replica division. Recently, Wang *et al.* reported a spatially and temporally DPA with an output pulse energy of 20 nJ, but the pulse duration was measured to be longer than 600 fs. An additional single-mode fiber (SMF) had to be employed to further compress the pulse, generating 7.3-nJ pulse energy in 96-fs pulse duration [16]. Furthermore, DPA in anomalous dispersion regime is still scientifically interesting because there are questions about the recombining efficiency when significant nonlinear phase is accumulated in the compression with a larger pulse compression ratio.

In this manuscript, we focus on exploring the potential of DPA at 1.55 μm. Fourier transform limited pulse with 126-fs pulse duration and 20.3-nJ pulse energy was directly obtained from the divided-pulse EDFA at 80-MHz. Experimentally, the combining efficiencies for 8, 16, and 32 replicas were measured. Moreover, double-check (frequency doubling to 780 nm and spectral broadening in an additional fiber) was applied to check the pulse peak power. Nearly 50% frequency-doubling efficiency is realized. By coupling a portion of output from DPA into an additional 20-cm polarization-maintaining single-mode fiber (PM-SMF), the pulses were further broadened in frequency domain and compressed to 65 fs.

2. Simulations

As for wavelength above 1.3 μm where laser pulses travel in anomalous dispersion regime of optical fiber, pulse amplification and compression may be simultaneously carried out so that no separate compressors are required [24], [25]. Intuitively, for simultaneous pulse amplification and compression in EDFAs, a positively pre-chirping seed pulse is desired. Through normal dispersion fiber, the initial pulse emitting from a mode-locked laser acquires a chirp, while its spectral shape

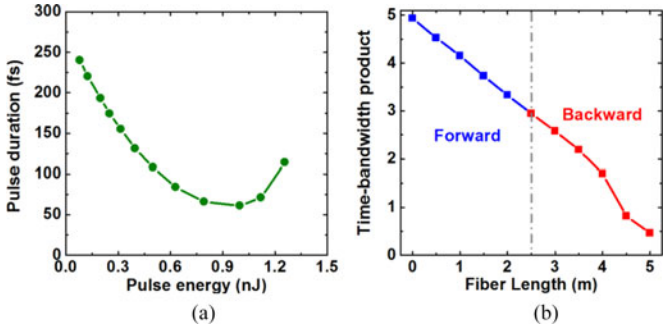

Fig. 1. Simulation results. (a) Pulse duration as a function of pulse energy. (b) Time-bandwidth product at different position of the fiber amplifier. The blue and red curves represent forward and backward amplification in the double-pass fiber amplifier, respectively.

remains unchanged (if nonlinearity can be neglected). Such a pre-chirping can keep sufficient low peak power at the beginning of pulse amplification and thus help to acquire enough gain. In order to study such nonlinear compression of active fiber in anomalous dispersion regime, the generalized nonlinear Schrödinger equation (GNLSE) with the split-step Fourier method were used to simulate pulse propagation [26]. Pulse with 2.0-ps temporal duration, 19.9-nm spectral width (corresponding to 0.13 ps^2 pre-chirping on 180 fs transform-limited pulse), and 0.05-nJ pulse energy was applied as the seed laser, and a 5.0-m-long active fiber with group velocity dispersion (GVD) of -23 fs^2/mm and nonlinear coefficient of 2 $W^{-1}\cdot km^{-1}$ performed the simulations.

Simulation results are shown in Fig. 1. It clearly shows that there exists an equilibrium position which can not only restrict excessive nonlinear effects to ensure high-quality temporal integrity, but also produce sufficient optical nonlinearity to broaden the spectrum to support $<$100 fs pulse duration. The shortest pulse duration of 64 fs is achieved with an optimized pulse energy of 1 nJ [see Fig. 1(a)]. While in the case of no laser gain, the incident pulse can be only compressed to 240 fs by the anomalous dispersion. Fig. 1(b) shows the time-bandwidth product (TBP) evolution of the shortest pulse along the double-pass fiber amplifier. The TBP decreases linearly in both forward and backward direction, from positively-chirped pulse with TBP of 4.9 at the input port to nearly transform-limited pulse with TBP of 0.46 at the output port.

3. Experimental Setup and Results

A stretched pulse fiber oscillator provided the seed pulse with 80-MHz repetition rate. A pre-amplifier was used to preliminarily amplify and positively pre-chirp the seed pulse to a duration of 2.4 ps. The pre-chirped pulse was divided by a hybrid divider and then was recombined with the help of a FRM reflecting pulses to pass through the same series (see Fig. 1). As depicted in the inset of Fig. 2, three YVO_4 crystals 2^1, 2^2, and 2^3 with lengths of 10, 20, and 40 mm divided the initial pulse into eight replicas. In the consideration of the expensive price, optical quality and assemblability for YVO_4 crystals longer than 80 mm, PBSs acted as 2^4 and 2^5 dividers.

The system firstly operated with three YVO_4-based dividers. The combined and uncombined powers at the corresponding output port A and B are plotted along with the combining efficiency as a function of pump power [see Fig. 3(a)]. It clearly shows that the efficiency drops as the pump power increases. With 8 replicas, the combining efficiency starts at 99.5% and remains above 95% in moderate-nonlinearity regime where pump power is less than 4 W. Subsequently, the combined fraction gradually tends to be saturated and the uncombined fraction rapidly increases in over-nonlinearity regime where pump power is higher than 4 W, and the corresponding combining efficiency decays to 80% at 7-W pump power.

To investigate the recombination process in this fiber amplifier, the spectral width (AQ6370, Yokogawa) and autocorrelation traces (pulse check SM1200, APE) were recorded at the combined and uncombined output ports. As pump power increased within moderate-nonlinearity regime, SPM

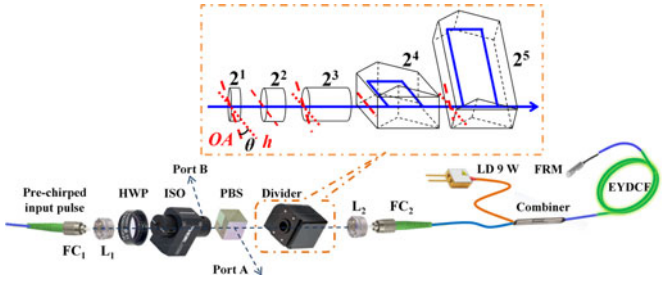

Fig. 2. Experiment setup. FC1 and FC2: fiber connectors. L1 and L2: lens. HWP: half-wave plate. ISO: isolator. PBS: polarization beam splitter cube. LD: laser diode with 9 W output power. EY-DCF: 12/130 Erbium-Ytterbium codoped double-clad fiber with numerical aperture of 0.2 for the fiber core and 0.46 for the cladding. FRM: Faraday rotator mirror. (Inset) Scheme of the divider: the in-line YVO_4-based stages as well as the PBS-based stages. 2^N represents the stage order. The red dash line OA, red dot line h, and θ represent crystal optical axis, horizontal line, and angle between them, respectively.

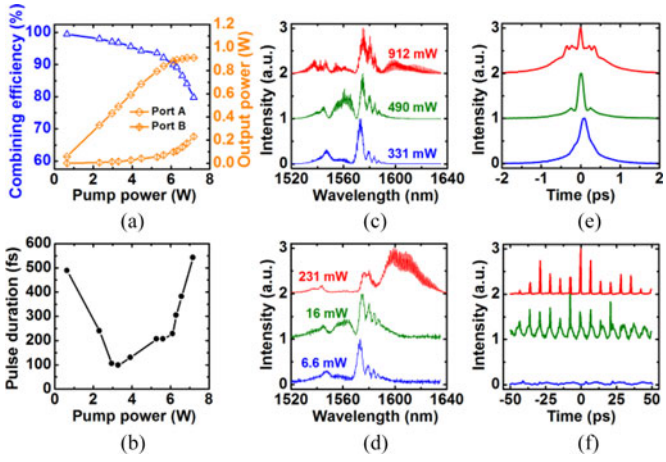

Fig. 3. (a) Output powers at port A and port B, as well as combining efficiency as a function of pump power for eight replicas. (b) The pulse duration as a function of pump power. The output spectra at port A (c) and port B (d) with 2.3-W (blue), 3.3-W (green), and 7.2-W (red) pump power, respectively. The number close to the spectrum represents the output power of the corresponding curve. The autocorrelation traces of pulse at port A (e) and port B (f) with 2.3-W (blue), 3.3-W (green), and 7.2-W (red) pump power. Output power less than 10 mW is too low to be detected in the autocorrelator, respectively.

broadened the spectrum, and simultaneously, the anomalous dispersion of the fiber compressed the new spectral components, resulting in temporal shortening. Before breaking up, the pulse reached its shortest duration of 98 fs [see the green curve in Fig. 3(e)] with 490-mW average output power (6.1-nJ pulse energy), corresponding to pulse compression ratio of up to 25. Here, counting the uncombined energy at port B, the total energy per replica is calculated to be 0.79 nJ. At this energy level, the combined and uncombined fractions exhibit almost identical spectra [see the green curves in Fig. 3(c) and (d)], and the combining efficiency is as high as 96.8%, indicating that the new spectral components do not obviously degrade the combining efficiency but maintain good coherence. The 2.7% decrement in combining efficiency can be partially attributed to the imperfect pulse division in amplitude of each replica and the consequent accumulated phase difference. Although the average power of uncombined fraction is only 16 mW, it is sufficient to distinguish the uncombined replicas in the autocorrelation trace, shown as the green curve in Fig. 3(f).

However, in the over-nonlinearity regime where pump power is higher than 6 W, stimulated Raman scattering (SRS) played a very apparent role in spectral broadening [see the red curves in Figs. 3(c) and (d)], and pulse break up occurred inevitably [see the red curve in Fig. 3(e)]. The red-shift spectrum accounted for a large proportion of the energy at port B and degraded the combining

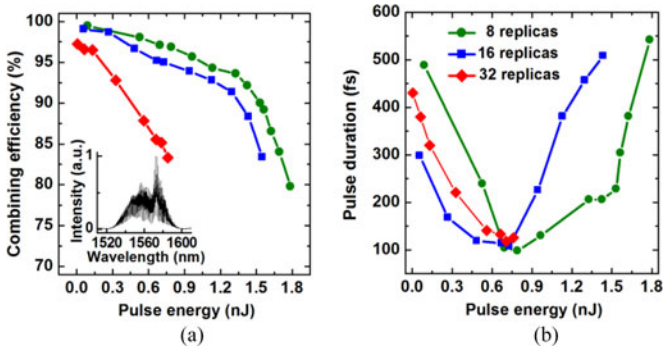

Fig. 4. (a) Combining efficiency as a function of energy per replica for eight (green), 16 (blue), and 32 (red) replicas, respectively. (Inset) Spectrum of at port B with 16 replicas. (b) Pulse duration as a function of energy per replica for eight (green), 16 (blue), and 32 (red) replicas, respectively.

efficiency to 80%. This is easily understood because higher nonlinearity and the accordingly large different phase shift make the new spectral components of each replica hardly recombine. This degradation in coherency is also visible by comparing the combined and uncombined spectra. At this energy level per replica ($\sim$1.8 nJ), obvious spectral interference could be observed from the uncombined output. The modulation across the spectra had a period of 1.2 nm, corresponding to a 6.7 ps time delay (matching well with the polarization-mode delay of 10-mm-long YVO_4 crystal), and could be identified as the result of the imperfect recombination process. In addition, the imperfect temporal feature could be further identified by the measured autocorrelation traces [see the red curve in Fig. 3(f)]. It can be seen that the pedestal dramatically grows for high output power. We believed it might be mainly caused by the SPM in the anomalous fiber amplifier. Because the GVD-induced chirp is linear and SPM-induced chirp is far from being linear across the entire pulse in time domain, the red-shifted light near the leading edge is overtaken by the blue-shifted light as well as the unshifted light in anomalous dispersion fiber. As a result for pulse energy above 1 nJ, the energy in the pulse tail spreads out, and the pulse acquires pedestal and thus broadens. Therefore, over-nonlinearity (especially SRS) is the main limitation on pulse energy extracted from the $\times$8 DPA.

To extract more energy from the double-pass amplifier, we increased the number of the replicas from 8 to 16 and 32. As shown in the inset of Fig. 2, the additional 2^4 and 2^5 divisions were implemented by adding PBS-based dividers just behind the YVO_4-based dividers on the beam pass. The p-polarized components (parallel to the top of PBS 2^4) were transmitted while the s-polarized components (perpendicular to the top of PBS 2^4) were reflected to the delay line. By reflecting twice in the rectangular prism, the delayed pulse was reflected in the direction of the initially transmitted pulse. The 2^5 PBS-based divider oriented at an angle of 45° to the horizontal plane. In order to avoid the difficulty in optical alignment and improve the compactness, we used monolithic fused-silica as the delay line. Owing to the delay length of 26.8 and 53.6 mm, the 2^4 and 2^5 stages provided time delay of 130 and 260 ps, respectively. Therefore, this hybrid divider divided the input pulse to 16 (32) replicas, leading to two (four) 50-ps envelops with 130-ps interval.

To gain more insight on the recombination process, we measured the combining efficiency for different number of replicas. The results for 16 and 32 replicas as well as 8 replicas for comparison are displayed in Fig. 4. When 16 replicas are generated, the combining efficiency starts at 99% and remains above 95% in moderate-nonlinearity regime where energy per replica is less than 0.75 nJ. As pump power increases, the combined fraction tends to be saturated at an average power of 1.6 W and the uncombined fraction increases rapidly when pump power is higher than 6 W. The output powers with the shortest pulse duration of 108 fs are measured to be 890 and 46.8 mW at port A and B, respectively. Due to the increase in the number of pulses, distinct spectral interferences appear over the whole spectrum at the uncombined output port [see the inset of Fig. 4(a)]. Obvious decrease of combining efficiency is observed when 32 replicas are applied. The

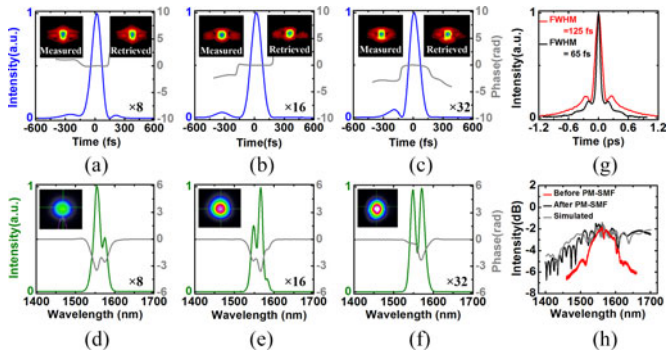

Fig. 5. Retrieved FROG temporal (blue curves) and phase (gray curves) intensities of laser pulses from the main amplifier for $\times 8$ (a), $\times 16$ (b), and $\times 32$ (c) replicas. (Insets) Measured and retrieved FROG patterns, respectively. The retrieved FROG spectral (green curves) and phase (gray curves) intensities of laser pulses from main amplifier for $\times 8$ (d), $\times 16$ (e), and $\times 32$ (f) replicas. (Insets) Measured beam patterns frequency-doubled to 780 nm. (g) Measured autocorrelation traces before (red curve) and after (black curve) the additional 20-cm PM-SMF. (h) Measured spectrum before (red curve) and after (black curve) the additional PM-SMF, as well as simulated spectrum (gray curve).

combining efficiency starts at 97.2% and decays to 83.3% when energy per replica is 0.76 nJ. The output powers with the shortest pulse duration of 126 fs are measured to be 1.62 W and 326 mW at port A and B, respectively. It is worth noting that the combining efficiency for 32 replicas decays so fast is a result of shorter seed pulse. When the number of replicas increases, replica with insufficient energy cannot produce enough spectral bandwidth to support 100-fs pulse. Thus, a shorter seed pulse with 2.2-ps duration is preferred in the setup for 32 replicas. The benefits of shorter seed pulse decreased the length of fiber in the double-pass fiber amplifier in which high-order dispersion and other nonlinearity (such as SRS) could be minimized.

4. Discussions

Interestingly, in our experiment, $\sim$0.75-nJ energy is the best value for transform-limited pulse generation [see Fig. 4(b)]. This is because the transform-limited replica is produced as a result of the interplay between the dispersive and nonlinear effects, and in such a way soliton forms. Considering a fixed value of net GVD in double-pass fiber amplifier, the energy per replica steadily increases and gradually approaches to a same value when the pump power increases. In other words, no matter how many replicas are generated, the energy per replica is a fixed value in the identical nonlinear fiber amplifier. Fig. 5(a)–(f) show the retrieved temporal and spectral intensities (15-40-USB, Swamp optics) of the recombined pulse at this optimized pulse energy. As shown in the insets of Fig. 5(a)–(c), the measured and retrieved FROG patterns matched very well for different division, respectively. As predicted in previous simulation, replica reaches its shortest pulse with 1-nJ energy. The differential in energy probably comes from the splicing loss between different type fibers (0.6 dB) and the insertion loss of Faraday reflection (0.6 dB).

Two effects limited the energy per replica to $\sim$1 nJ. First, considering the available seeding energy, higher pump power leads to CW oscillation in the amplifier and thereupon results in output power instability. Second, for the active fiber with 130 μm cladding diameter, efficient heat dissipation has to be considered when pump power is higher than 15 W.

Differential GVD between two orthogonal polarizations of the YVO_4 crystal is the main limitation on $<$120 fs pulse generation. Generally, the differential GVD of YVO_4 has a typical value of 55 fs^2/mm at 1560 nm (92 and 147 fs^2/mm for ordinary and extraordinary axes, respectively). For the divider with three YVO_4 crystals (10, 20, and 40 mm), the differential GVD is about 1650 fs^2 (equivalent to 30-mm-length YVO_4). Considering transform-limited replicas with 40-fs duration to carry out the recombine process, 1650 fs^2 differential GVD would stretch the pulse duration to

121 fs. Therefore, the length of YVO_4 crystals should be as short as possible as long as successive replicas do not overlap.

A PPLN with 20.9-μm poling period and 0.3-mm length was used for frequency-doubling the amplified laser and checking its peak power. A pair of lens were used to focus and collimate the input and output beam on the PPLN, respectively. Optimization of the laser produced stable average output powers of 247.5, 302, and 472 mW at 785 nm with 490, 550, and 973 mW incident power at the fundamental repetition rate, corresponding to 50.5%, 54.9%, and 48.5% for $\times$8, $\times$16, and $\times$32 replicas, respectively. To avoid facet damage on PPLN, the incident laser pulse at 1560 nm are limited to 1-W average power. We analyze the beam quality at the output of the PPLN for different replicas, as shown in the insets of Fig. 5(d)–(f). The beam quality for $\times$32 replicas is slightly poorer than those of $\times$8 and $\times$16 replicas because of spatial interference.

Furthermore, an additional PM-SMF was used to verify the achieved peak power from the DPA with $\times$32 replicas. In order to avoid damage on fiber end face, a portion of output pulse train was coupled into 20-cm PM-SMF. Owing to the co-effect of nonlinearity and GVD, the pulses were further broadened in frequency domain and compressed in time domain. The red and black curves shown in Fig. 5(g) present the autocorrelation traces before and after the additional PM-SMF. The shortest pulse duration of 65 fs was obtained with 570-mW coupling average power. Moreover, a simulation using the GNLSE (GVD $= 23$ fs^2/mm, $\gamma = 2$ W^{-1}·km^{-1}, pulse energy of 7 nJ) was carried out. The envelop of the measured and simulated spectrum match well, shown as the black and gray curves in Fig. 5(h). For comparison, the incident spectra are also presented as the red curve in Fig. 5(h).

In conclusion, we propose a polarization-division-multiplexing scheme to mitigate the nonlinearity in EDFA. By generating and recombining 32 replicas, pre-chirped laser pulses were amplified to 20.3-nJ pulse energy and simultaneously compressed to 126-fs duration, corresponding to a peak power of 161 kW. Quantitative measurements and analyses of the combining efficiency for different number of replicas are discussed. Power scaling at 1560 nm is currently limited by thermal-induced damage on optical fibers and fiber components. These are technical issues that can be solved with careful thermomechanical design as well as high power fiber components. Therefore, higher pulse energy and average power can be expected when 64 and 128 replicas are applied. In the near future, compressor-free power amplification to 100-nJ pulse energy with $\sim$100-fs duration (corresponding to 1-MW peak power) at 1560 nm might be achieved by using seed pulses at 10-MHz repetition rate.

References

[1] F. Morin, F. Druon, M. Hanna, and P. Georges, "Microjoule femtosecond fiber laser at 1.6 μm for corneal surgery applications," *Opt. Lett.*, vol. 34, pp. 1991–1993, Jun. 2009.

[2] C. Lee, S. T. Chu, B. E. Little, J. Bland-Hawthorn, and S. Leon-Saval, "Portable frequency combs for optical frequency metrology," *Opt. Exp.*, vol. 20, pp. 16671–16676, Jul. 2012.

[3] C. Lee *et al.*, "Pre-Chirped pulse excitation enhanced terahertz radiation," *IEEE T. THz Sci. Tech.*, vol. 6, pp. 253–261, Mar. 2016.

[4] J. R. Unruh, E. S. Price, R. G. Molla, L. Stehno-Bittel, C. K. Johnson, and R. Hui, "Two-photon microscopy with wavelength switchable fiber laser excitation," *Opt. Exp.*, vol. 14, pp. 9825–9831, Sep. 2006.

[5] M. Hofer, M. E. Fermann, A. Galvanauskas, D. Harter, and R. S. Windeler, "High-power 100-fs pulse generation by frequency doubling of an erbium ytterbium-fiber master oscillator power amplifier," *Opt. Lett.*, vol. 23, pp. 1840–1842, Dec. 1998.

[6] G. Imeshev, I. Hartl, and M. Fermann, "An optimized Er gain band all-fiber chirped pulse amplification system," *Opt. Exp.*, vol. 12, pp. 6508–6514, Dec. 2004.

[7] V. Roy, L. Desbiens, and Y. Taillon, "All-fiber high power rugged ultrashort-pulse laser source at 1550 nm," in *Proc. SPIE*, vol. 7386, May 2009, Art. no. 738633.

[8] I. Pavlov, E. Ilbey, E. Dülgergil, A. Bayri, and F. Ö. Ilday, "High-power high-repetition-rate single-mode Er-Yb-doped fiber laser system," *Opt. Exp.*, vol. 20, pp. 9471–9475, Apr. 2012.

[9] J. W. Nicholson *et al.*, "Scaling the effective area of higher-order-mode erbium-doped fiber amplifiers," *Opt. Exp.*, vol. 20, pp. 24575–24584, Oct. 2012.

[10] J. W. Nicholson *et al.*, "Axicons for mode conversion in high peak power, higher-order mode, fiber amplifiers," *Opt. Exp.*, vol. 23, pp. 33849–33860, Dec. 2015.

[11] Z. Várallyay and J. C. Jasapara, "Comparison of amplification in large area fibers using cladding-pump and fundamental-mode core-pump schemes," *Opt. Exp.*, vol. 17, pp. 17242–17252, Sep. 2009.

[12] S. Ramachandran, "Dispersion-tailored few-mode fibers: A versatile platform for in-fiber photonic devices," *J. Lightw. Technol.*, vol. 23, no. 11, pp. 3426–3443, Nov. 2005.
[13] S. Zhou, F. W. Wise, and D. G. Ouzounov, "Divided-pulse amplification of ultrashort pulses," *Opt. Lett.*, vol. 32, pp. 871–873, Apr. 2007.
[14] E. S. Lamb, L. G. Wright, and F. W. Wise, "Divided-pulse lasers," *Opt. Lett.*, vol. 39, pp. 2775–2777, May 2014.
[15] Q. Hao *et al.*, "Divided-pulse nonlinear amplification and simultaneous compression," *Appl. Phys. Lett.*, vol. 106, Mar. 2015, Art. no. 101103.
[16] C. Wang, W. Li, L. Li, Q. Hao, J. Zhao, and Heping Zeng, "Femtosecond Er-doped fiber laser based on divided-pulse nonlinear amplification," *J. Opt.*, vol. 18, Jan. 2016, Art. no. 025503.
[17] L. J. Kong, L. M. Zhao, S. Lefrancois, D. G. Ouzounov, C. X. Yang, and F. W. Wise, "Generation of megawatt peak power picosecond pulses from a divided-pulse fiber amplifier," *Opt. Lett.*, vol. 37, pp. 253–255, Jan. 2012.
[18] M. Kienel *et al.*, "Analysis of passively combined divided-pulse amplification as an energy-scaling concept," *Opt. Exp.*, vol. 21, pp. 29031–29042, Nov. 2013.
[19] M. Kienel, A. Klenke, T. Eidam, S. Hädrich, J. Limpert, and A. Tunnermann, "Energy scaling of femtosecond amplifiers using actively controlled divided-pulse amplification," *Opt. Lett.*, vol. 39, pp. 1049–1052, Feb. 2014.
[20] J. C. Jasapara, M. J. Andrejco, J. W. Nicholson, A. D. Yablon, and Z. Várallyay, "Simultaneous direct amplification and compression of picosecond pulses to 65-kW peak power without pulse break-up in erbium fiber," *Opt. Exp.*, vol. 15, pp. 17494–17501, Dec. 2007.
[21] F. Guichard *et al.*, "Energy scaling of a nonlinear compression setup using passive coherent combining," *Opt. Lett.*, vol. 38, pp. 4437–4440, Nov. 2013.
[22] A. Klenke, M. Kienel, T. Eidam, S. Hädrich, J. Limpert, and A. Tünnermann, "Divided-pulse nonlinear compression," *Opt. Lett.*, vol. 38, pp. 4593–4596, Nov. 2013.
[23] F. Guichard, M. Hanna, Y. Zaouter, D. N. Papadopoulos, F. Druon, and P. Georges, "Analysis of limitations in divided-pulse nonlinear compression and amplification," *IEEE J. Sel. Topics Quantum Electron.*, vol. 20, Sep./Oct. 2014, Art. no. 7600405.
[24] J. Takayanagi *et al.*, "Generation and detection of broadband coherent terahertz radiation using 17-fs ultrashort pulse fiber laser," *Opt. Exp.*, vol. 16, pp. 12859–12865, Aug. 2008.
[25] D. A. Gaponov *et al.*, "High power all-fibered femtosecond master oscillator power amplifier at 1.56 μm," *Opt. Lett.*, vol. 37, pp. 3186–3188, Aug. 2012.
[26] G. P. Agrawal, *Nonlinear Fiber Optics*, 5th ed. New York, NY, USA: Academic, 2013.